

15th Water-Rock Interaction International Symposium, WRI-15

# Numerical simulation of CO<sub>2</sub> injection into a carbonate aquifer: implications of fluid–rock reactions in the aquifer and in an overlying clay formation

Peter Alt-Epping<sup>a,\*</sup>, Larryn W. Diamond<sup>a</sup>

<sup>a</sup>*Rock-Water Interaction Group, Institute of Geological Sciences, University of Bern, Bern, Switzerland*

---

## Abstract

We use reactive transport simulations to evaluate the CO<sub>2</sub> sequestration potential of a carbonate-hosted aquifer. Results show that in carbonate aquifers the dissolution of CO<sub>2</sub> into the brine is the only effective chemical trapping mechanism. Its efficiency is controlled by the solubility of CO<sub>2</sub> and by the mobility of the CO<sub>2</sub> plume which affects its size and shape and thus the contact area between the plume and the brine. Porosity and permeability changes following CO<sub>2</sub> injection are small and have little effect on the injectivity or the mobility of the plume. The model is extended to examine processes at the aquifer/seal interface and within the clay formation following the rise of the CO<sub>2</sub> plume towards the seal. Reactive transport simulations include diffusion and electromigration into the clay and involve a new method for an explicit treatment of a diffuse layer on charged clay mineral surfaces. Simulations show that the diffuse layer exerts a strong impact on the breakthrough of the CO<sub>2</sub>-enriched, acidic plume into the clay as it influences all species as a function of their charge. The local pore water composition and mineral solubilities in the clay are affected, leading to patterns that cannot be predicted by conventional ion-exchange models.

© 2017 Published by Elsevier B.V. This is an open access article under the CC BY-NC-ND license

(<http://creativecommons.org/licenses/by-nc-nd/4.0/>).

Peer-review under responsibility of the organizing committee of WRI-15

*Keywords:* CO<sub>2</sub> sequestration; reactive transport; electromigration

---

## 1. Introduction

A study by<sup>7</sup> has identified several deep saline aquifers in the Swiss Molasse Basin, which may potentially be used as reservoirs to sequester industrial CO<sub>2</sub> emissions. Most of these potential target aquifers are composed of carbonate rocks. Here we focus on the Trigonodus Dolomite aquifer, a 30–40 m thick, porous unit of the Triassic Upper Muschelkalk formation that is underlain by the Hauptmuschelkalk, a tight limestone, and

---

\* Corresponding author. Tel.: +41 31 631 4531; fax: +41 31 631 4843.

E-mail address: [alt-epping@geo.unibe.ch](mailto:alt-epping@geo.unibe.ch)

overlain by a clay-rich formation of the Gipskeuper, which would trap the rising CO<sub>2</sub> plume. To further evaluate its storage capacity, injectivity and long-term isolation performance, predictive numerical simulations have been carried out, constrained by experimental and observational data.

Simulations show that injection into carbonate aquifers is different from injection into silicate-hosted aquifers in terms of chemical trapping capacity. Consequently, special care needs to be taken to ensure the long-term integrity of the seal. Thus, in the second part of this paper we will look at processes taking place at the aquifer/seal interface. To assess these processes we explicitly account for effects related to the electrical double-layers that form at clay mineral surfaces. Electrostatic interaction between the pore water and the clay mineral surface and the effect on the local fluid composition has become an important issue in research on nuclear repositories<sup>1</sup>. Here we use reactive transport simulations to study this effect in the context of CO<sub>2</sub> sequestration.

## 2. CO<sub>2</sub> injection into the Trigonodus Dolomite

### 2.1. Modelling approach

We use the code PFLOTRAN<sup>4</sup> ([www.pflotran.org](http://www.pflotran.org)) to conduct simulations of CO<sub>2</sub> injection into the Trigonodus Dolomite. PFLOTRAN uses a kinetic formulation for mineral dissolution and precipitation reactions based on transition-state theory. Kinetic parameters such as the rate constant and activation energies used in this study are taken from<sup>5</sup>. Reactive surface areas of minerals are poorly known and here we choose a somewhat arbitrary  $1 \text{ m}^2 \text{ m}^{-3}_{\text{bulk}}$  for all minerals in the system. Carbonate and sulphate minerals generally exhibit fast reaction rates leading to local equilibrium. Hence, detailed knowledge of the reactive surface area is not required if local equilibrium conditions have been attained. Water retention properties of the Upper Muschelkalk are taken from<sup>2</sup>.

We use a simple axisymmetric model which is 2 km in diameter and consists of 40 m of Hauptmuschelkalk overlain by 35 m of Trigonodus Dolomite. Top and bottom boundaries are impermeable and along the side boundaries a hydrostatic pressure is assigned. We assume homogeneous rock properties throughout the Hauptmuschelkalk and the Trigonodus Dolomite. Both units are composed of calcite, dolomite and accessory anhydrite, whereby dolomite is dominant in the Trigonodus Dolomite and calcite in the Hauptmuschelkalk. The initial porewater has a salinity of 0.5 mol/kg and is in equilibrium with the primary mineral assemblage. It is known from laboratory experiments that the porosity and intrinsic matrix permeability of the Trigonodus dolomite are around 0.15 and  $1\text{e-}15 \text{ m}^2$ , respectively. However, the Trigonodus dolomite is locally fractured, such that in-situ hydraulic tests yield formation-scale permeabilities up to  $5\text{e-}14 \text{ m}^2$ . For the Hauptmuschelkalk we use a porosity and permeability of 0.05 and  $5\text{e-}17 \text{ m}^2$ , respectively.

### 2.2. Chemical trapping of CO<sub>2</sub> in carbonate aquifers

Solubility trapping occurs via dissolution of CO<sub>2,sc</sub> into H<sub>2</sub>O. The dissolution process leads to a sequence of aqueous reactions that release acidity and bicarbonate. The release of acidity affects, among others, the stability of carbonate minerals. Furthermore, bicarbonate may bond with cations and precipitate as carbonate minerals, thus trapping CO<sub>2</sub> in solid form, which is the safest and most desired form of chemical CO<sub>2</sub> trapping. As CO<sub>2</sub> is injected the plume expands and moves upwards as a result of buoyancy forces caused by the density difference between CO<sub>2</sub> and the formation brine. We assume that there are no hydraulic gradients causing the plume to move with the groundwater flow. The upward movement of the plume continues until it encounters a low-permeability cap rock, which is represented in the model as a no-flow boundary at the top of the domain. The low-permeability seal forces the plume to spread laterally. Along its edges, CO<sub>2</sub> continues to dissolve into the brine, leading to a local increase in density of the aqueous phase and initiating finger-like downward convection of the CO<sub>2</sub>-enriched brine (Figure 1A).

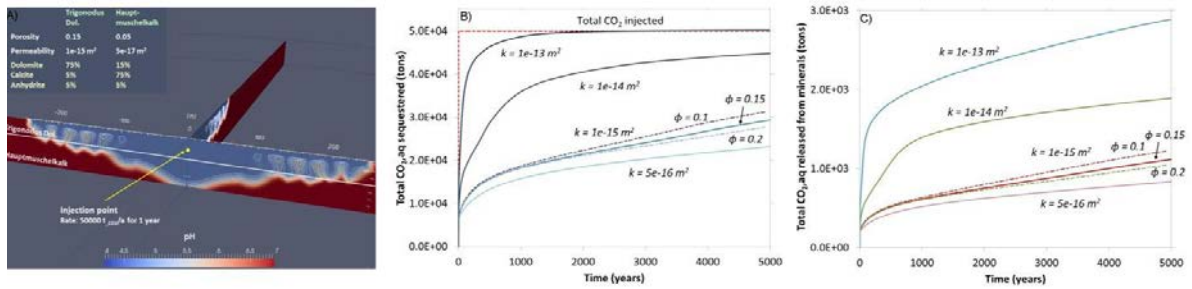


Figure 1 Panel (A): The CO<sub>2</sub> plume after 5000 years for an aquifer permeability of 1e-15 m<sup>2</sup> represented as a region of low pH. Panel (B): A high permeability and lower porosity are favorable for trapping CO<sub>2</sub> via dissolution into the brine. Panel (C): CO<sub>2</sub> injection into carbonate aquifers involves the dissolution of carbonate minerals and a release of additional CO<sub>2</sub>.

Global mass balance calculations show that the rate of solubility trapping is highest during the early, most mobile phase of the plume, when pressure gradients and buoyancy forces are strongest (Figure 1B). The rate tends to decrease after shut-in when pressures recover and the plume no longer expands. The rate of solubility trapping is strongly dependent on the aquifer permeability which controls the mobility of the plume as well as its size and shape and hence the contact area between CO<sub>2,sc</sub> and the brine. It depends to a lesser degree on porosity. The higher the permeability, the larger the surface contact area of the plume and the higher the trapping capacity (Figure 1B).

The acidification of the brine induces carbonate mineral dissolution, which constitutes an additional source for CO<sub>2,aq</sub>. Thus, the dissolution of minerals lowers the solubility trapping capacity. The amount of CO<sub>2</sub> released from dissolved minerals correlates with the aquifer permeability: a higher permeability implies a higher total mass of dissolved carbonate minerals. However, the CO<sub>2,aq</sub> released from mineral dissolution contributes only a small portion to the total amount of dissolved CO<sub>2</sub> in the brine (Figure 1C). Thus, the dissolution of CO<sub>2</sub> still constitutes an effective trapping mechanism, whereby a high permeability of the aquifer rock is generally favorable. The small amount of carbonate dissolution implies virtually no change in the hydraulic properties of the aquifer rock.

### 3. Processes at the aquifer–seal interface

Given that solubility trapping is the only effective chemical trapping mechanism in carbonate hosted aquifers, the long term integrity of the seal needs to be ensured. Simulating solute transport through clay is complicated by the fact that clay minerals may exhibit a negative surface charge, forming a diffuse layer of excess cations adjacent to mineral surfaces known as the electrical double-layer (EDL). With increasing distance from the mineral surface the electrical potential decreases until at infinite distance the pore water becomes internally charge-balanced. The pore water unaffected by surface charge is referred to as free water. The concept of anion-accessible porosity as part of the total porosity has been inferred from experiments on clay materials<sup>6</sup>.

A 1D model is used to represent the contact between a carbonate aquifer and an overlying clay unit patterned after the Opalinus Clay in Switzerland. The total length of the 1D domain is 10 m, a section of 0.5 m constitutes the aquifer and the remaining 9.5 m represent the clay. Both rocks have the same total porosity of 0.15. In the clay the total porosity is divided into a fraction containing free water and a fraction with EDL pore water making up 0.05 and 0.1, respectively. The clay exhibits a cation exchange capacity of 11.1 meq/100g<sub>rock</sub>. We use a generic clay mineral to represent the exchanger. The exchanger is inert. Diffusion coefficients are species-dependent and are taken from<sup>1</sup>. For the aquifer we assume an effective diffusion coefficient ( $D_e$ ) for an uncharged tracer of 1e-10 m<sup>2</sup>/s. In the free water the same uncharged tracer exhibits a  $D_e$  of 2.5e-11 m<sup>2</sup>/s. Species in the EDL have effective diffusivities which are a factor of three lower than in the free water. Both the aquifer and the clay contain only calcite as a reactive mineral. The initial pore water in the aquifer and in the clay is at calcite equilibrium with initial pCO<sub>2</sub> = 0.01 bar and salinity of 0.5 molar NaCl. We use the approach by<sup>3</sup> to maintain Donnan equilibrium between the EDL and the free water at all times. We run the simulation to 100 years to eliminate any transients induced by the initial conditions. After 100 years the CO<sub>2</sub> plume approaches the clay, perturbing the initial Donnan equilibrium conditions. The arrival of the CO<sub>2</sub> plume is simulated by increasing the pCO<sub>2</sub> in the aquifer to 100 bars. Single-

phase conditions are assumed. For comparison we run an additional simulation of diffusion into a hypothetical uncharged clay without EDL. For this case we assume for the clay a total porosity of 0.15 and the same pore diffusion coefficient as for the free water in the scenario involving an EDL.

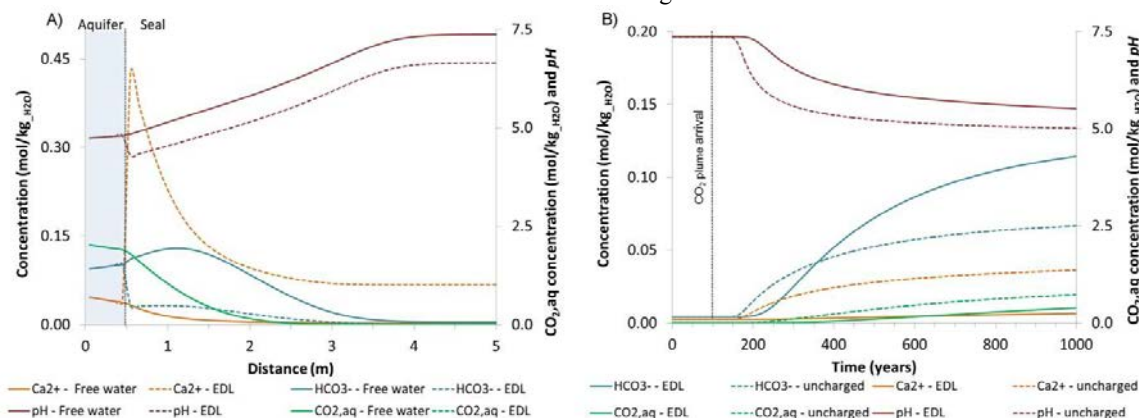


Figure 2 Panel A) shows spatial profiles of concentrations of selected species in the free water and in the EDL 50 years after the arrival of the plume. Panel B) shows breakthrough curves at an observation point in the free water 4.5 m into the clay.

Figure 2A shows the concentration profiles of selected species 50 years after the arrival of the CO<sub>2</sub> plume at the aquifer/seal contact. The arrival is marked by a strong increase in CO<sub>2</sub> and acidity in the aquifer groundwater. The pH decreases from an initial value of 7.36 to around 4.7. Calcite dissolves releasing Ca<sup>2+</sup> into the groundwater. Calcium diffuses into the clay, initiating the exchange with Na<sup>+</sup> in the EDL. The tendency of Ca<sup>2+</sup> to move into the EDL leads to the dissolution of calcite in the clay, which in turn releases Ca<sup>2+</sup> and bicarbonate. The exchange leads to a retardation of the Ca<sup>2+</sup> breakthrough (Figure 2B). In contrast, the charge-neutral CO<sub>2,aq</sub> is distributed evenly between the EDL and the free water (Figure 2A). The negatively charged bicarbonate diffuses preferentially in the free water such that its diffusive flux from the aquifer into the clay is lower than that of other species. Similarly to Ca<sup>2+</sup>, but at lower concentrations, H<sup>+</sup> ions move preferentially into the EDL, thus contributing to exchange reactions leading to a pH contrast between the EDL and the lower pH free water. Dissolved CO<sub>2,aq</sub> reacts with H<sub>2</sub>O to form bicarbonate and acidity. In the EDL, bicarbonate ions that form upon entry of CO<sub>2,aq</sub> are expelled from the EDL, leading to a strong enrichment in HCO<sub>3</sub><sup>-</sup> in the free water, thereby enhancing the pH contrast. The HCO<sub>3</sub><sup>-</sup> concentrations are higher in the free water than in the aquifer, causing a backward diffusion of HCO<sub>3</sub><sup>-</sup> from the clay into the aquifer.

By explicitly considering electrical double-layers on clay mineral surfaces, all species undergo exchange reactions. The breakthrough and distribution of species is controlled by their charge. Although electrostatic effects seem less significant in the context of CO<sub>2</sub> sequestration as the charge-neutral CO<sub>2,aq</sub> is dominant, EDL models should be used in simulations demanding for a high degree of accuracy such as in repository research.

## References

1. Alt-Epping P, Tournassat C, Rasouli P, Steefel CI, Mayer KU, Jenni A, Mäder U, Sengor SS, Fernandez R, Benchmark reactive transport simulations of a column experiment in compacted bentonite with multispecies diffusion and explicit treatment of electrostatic effects. *Comp. Geosci.* 2014; doi:10.1007/s10596-014-9451-x.
2. André L, Azaroual M, Menjot A Numerical Simulations of the Thermal Impact of Supercritical CO<sub>2</sub> Injection on Chemical Reactivity in a Carbonate Saline Reservoir, *Transp Porous Med.*, 2010; **82**: 247–274
3. Gimmi, T. Simulating Donnan equilibrium in clays based on the Nernst-Planck equation. 2016 (in prep.)
4. Hammond GE, Lichtner PC, Field-Scale Model for the Natural Attenuation of Uranium at the Hanford 300 Area using High Performance Computing. *Water Resources Research*; **46**: Paper No. W09527. 2010; doi:10.1029/2009WR008819
5. Palandri J, Kharaka YK A compilation of rate parameters of water–mineral interaction kinetics for application to geochemical modeling. *US Geol. Surv. Open File Report 2004-1068*; 2004. 64 pp.
6. Van Loon LR, Glaus MA, Müller W, Anion exclusion effects in compacted bentonites: Towards a better understanding of anion diffusion. *Appl. Geochem.*, 2007; **22**, 2536-2552
7. Chevallier F, Feng L, Bösch H, Palmer PI, Rayner PJ, On the impact of transport model errors for the estimation of CO<sub>2</sub> surface fluxes from GOSAT observations. *Geophysical Research Letters*, **37**, L21803, doi:10.1029/2010GL044652, 2010.